Eco-Friendly Synthesis of Zerovalent Iron Nanoparticles in Carbon Nanofibers for Wastewater Treatment

Zafar Iqbal [*,†] , Giovanni Ausanio , Loredana Parlato , Giovanni Piero Pepe , Shahid Ali [†]

Posted Date: 23 October 2023

doi: 10.20944/preprints202310.1374.v1

Keywords: green tea extract; composite nanofibers; zerovalent iron nanoparticles; electrospinning technique; water filtration

Article

Eco-Friendly Synthesis of Zerovalent Iron Nanoparticles in Carbon Nanofibers for Wastewater Treatment

Z. Iqbal [1,2,*,†], G. Ausanio [1,2], L. Parlato [1,2], G. P. Pepe [1,2] and S. Ali [3,†]

[1] Department of Physics "Ettore Pancini", University of Naples Federico II, Monte Sant'Angelo, Via Cinthia 21, 80126 Naples, Italy
[2] CNR-SPIN and Department of Physics "Ettore Pancini", University of Naples Federico II, Piazzale Tecchio, 80, 80125 Naples, Italy
[3] Materials Research Laboratory, Department of Physics, University of Peshawar, Peshawar 25120, Pakistan
* Correspondence: zafar.iqbal@unina.it; Tel.: +39-3475508795
† Equal contributions.

Abstract: The presence of heavy metals in industrial effluents has recently become a source of concern for human health and the environment. Efficient removal of metal ions and wastewater treatment is essential for protecting public health and the environment. In this study, we present an eco-friendly, green synthesis of reactive and fully dispersed zerovalent iron nanoparticles (nZVI) in carbon nanofibers via an electrospinning technique. In this novel study, green tea (GT) was used as environmentally friendly, polyvinyl alcohol (PVA) was used for the stabilization and reduction of nZVI, and tetraethyl orthosilicate (TEOS) was added to provide flexibility and to increase the specific surface area of the nZVI based nanofibers. GT contains polyphenols, which act as reducing agents, converting iron ions into nZVI and the particles can then serve as the building blocks for the carbon nanofibers. TEOS can also contribute to the stability of the nZVI by coating their surfaces with a silica layer. This silica layer helps prevent the oxidation of the nZVI, thereby reducing their catalytic activity. The nZVI-based composite (~ 400 nm) / carbonized (~ 200 nm) nanofibrous mats were fully characterized by scanning electron microscopy. The average size of the nZVI embedded in the composite and carbonized nanofibers can range from 50 nm to 100 nm. The x-ray diffraction (XRD) analysis of nZVI-based carbon nanofibers showed that there is no crystallinity and a single-phase cubic structure. Both energy-dispersive X-ray spectroscopy (EDX) and Fourier transform infrared (FTIR) analysis also confirmed the formation of single-phase nZVI-based composite / carbonized nanofibers. The high intensity of the peaks in the FTIR spectrum indicates the formation of nZVI in the nanofibers structure. The electrospun nZVI-based carbon nanofibers have a higher surface area and better reactivity due to small particle size and large surface area-to-volume ratio. They can provide excellent water stability and dispersibility in water compared to bulk nZVI, which tend to agglomerate and settle quickly. Additionally, nanofiber morphology can enhance the mechanical strength and durability of the composite material. Due to low-cost synthesis and their high efficiency in removing pollutants, these nanofibers could be used as nano-filters for wastewater treatment.

Keywords: green tea extract; composite nanofibers; zerovalent iron nanoparticles; electrospinning technique; water filtration

1. Introduction

Recently, nZVI has attracted increasing scientific and technological attention because of its extensive applications in environmental remediation and wastewater treatment. By introducing nZVI into wastewater, it selectively targets and breaks down contaminants through a variety of chemical reactions. These reactions lead to the degradation or transformation of pollutants, resulting in improved water quality. Similarly, nZVI is also effective in detoxify wastewater pollutants such as bacteria and viruses and removing groundwater contaminants, including chlorinated organic compounds, pesticides, heavy metals, nitrates, and even uranium [1]. In the case of heavy metals such

 doi:10.20944/preprints202310.1374.v1

as lead, chromium, arsenic, mercury, and cadmium, nZVI can undergo redox reactions with metals ions, reducing them to fewer toxic forms that can be immobilized or removed from the water. Furthermore, nZVI can reduce nitrate and nitrite in wastewater through denitrification, converting them into nitrogen gas. This process helps in preventing eutrophication caused by excessive nutrient levels in water bodies. Moreover, nZVI is environmentally friendly itself, and combined with organic matter can increase its reactivity stability and delivery capacities in wastewater treatments and environmental remediations [2].

The nZVI is a promising material for wastewater treatment and environmental remediation due to its high reactivity toward various contaminants. They are commonly used as a reducing agent and are typically synthesized by reducing ferric and ferrous iron with sodium borohydride [3]. However, the synthesis and application of nZVI face challenges related to aggregation and sedimentation, which can affect its overall effectiveness in detoxifying contaminants [4]. Aggregation refers to the tendency of nZVI to come together and form larger clusters. This phenomenon occurs due to the high surface energy and reactivity of nZVI particles, leading to attractive forces between particles. Aggregation reduces the mobility and dispersibility of nZVI in wastewater, limiting its contact with contaminants. Sedimentation is the relatively high density of nZVI that tends to settle down or sediment in water or wastewater systems. This settling down of nZVI, resulting in reduced availability for contaminant degradation and decreased treatment efficiency.

To overcome the aggregation and sedimentation of nZVI and improve their reactivity and stability when used in porous media or environmental applications. Some synthetic methods and materials are being developed to produce more dispersible and stable nZVI or immobilizing in the membrane with a large surface to volume ratio. The polymers such as carboxymethyl cellulose or polyvinyl alcohol can be coated as a protective layer around nZVI and prevent their aggregation and improve stability [5]. Polar solvents, such as water or alcohol, are often used to facilitate the dispersion of nZVI particles. The choice of the solvents and proper control over properties during the synthesis of nZVI can influence its dispersibility and stability [6]. Rather than by synthesizing and stabilizing nZVI particles beforehand, another approach involves generating nZVI in situ at the site of application. In this method, a precursor compound, such as ferrous sulfate, is introduced into the system, and nZVI is formed in the presence of reducing agents. This approach ensures the immediate reactivity of freshly formed nZVI while avoiding issues related to particle aggregation [7]. nZVI particles can be immobilized onto support materials to improve their dispersibility and prevent settling. Support materials like activated carbon, silica, or porous polymers provide a matrix for nZVI particles, preventing their aggregation and enhancing their stability during application.

By employing the mechanisms or approaches related to the dispersibility and stability of nZVI can be significantly enhanced and more effective in wastewater treatment and environmental remediation. Zhang et al. demonstrated that the inclusion of humic acid improved the reactivity and stability of nZVI, increasing its trichloroethylene degradation efficiency [8]. Li et al. investigated the use of a biodegradable polymer, poly (lactic-co-glycolic acid) to modify nZVI. The modified nZVI showed enhanced stability and reactivity, resulting in higher removal efficiency of hexavalent chromium Cr (VI) as compared to unmodified nZVI [9]. In another study Zhang et al. showed that the nZVI-biochar composite exhibited enhanced reactivity and stability in the presence of natural organic matter, leading to improved trichloroethylene degradation efficiency [10]. Recently, Sun et al. used a polyvinyl alcohol-co-vinyl acetate-co-itaconic acid (PV3A) as a dispersant and synthesized a stable dispersive nZVI [11]. The PV3A stabilized nZVI had a relatively smaller mean size of 15.5 nm, whereas in the absence of PV3A, the formed nZVI had a mean size of 105.7 nm. He and Zhao have successfully synthesized nZVI with varied sizes using carboxy methyl cellulose as a stabilizer's agent, which feature prevents aggregations of nanoparticles [12].

Recently, the green synthesis of nZVI has been reported by many researchers using green tea extract which is a cheap and local resource. The green tea extract was chosen because of its biodegradability, being water-soluble at room temperature, and producing non-toxic products. Green tea extract, derived from the leaves of Camellia sinensis, are rich in polyphenols such as epigallocatechin gallate and catechins, which have high antioxidant properties. In this approach,

 doi:10.20944/preprints202310.1374.v1

Hoag et al. synthesized stable nZVI at room temperature by using green tea extract without the addition of any surfactants or polymers [13]. The polyphenols present in green tea leaves can promote the dispersibility of nZVI in aqueous environments, improving its mobility and potential for applications such as groundwater remediation. Furthermore, polyphenol acts as a reducing agent and a capping agent facilitating the reduction of iron to form stable nZVI particles and preventing aggregation. Ponder et al. successfully synthesized the stable nZVI with a diameter of 10-30 nm on a nonporous, hydrophobic polymer resin support. The synthesized nZVI exhibits a high reactivity toward the removal of metal ion contaminants in an aqueous solution [14].

The electrospinning technique is a simple and versatile synthesis method for producing various polymeric nanofibers and nanostructured materials with a high surface-to-volume ratio [15]. In this process an electric field is applied to a polymer solution, which leads to the formation of a jet that stretches and solidifies into nanofibers as it travels towards a grounded collector [16]. The produced nanofibers with extremely small diameters leading to large surface, enhanced interactions with contaminants in water and facilitating efficient adsorption and filtration. By controlling the parameters of the electrospinning process, such as polymer concentration, solution viscosity, and collection distance, the pore size of the nanofibers can be adjusted. The electrospun nanofibers possess excellent mechanical properties due to their aligned and interconnected fiber structure. This enhances the durability and robustness of the filter, making it more suitable for practical water filtration applications. For example, Xiao et al. fabricated nanofibrous mats by electrospinning a polymer solution containing a mixture of polyacrylic acid and polyvinyl alcohol and fibers incorporated with multi-walled carbon nanotubes to enhance their mechanical durability [17]. The hybrid nanofibrous mats were used as supporting material for zerovalent iron nanoparticles, used for the remediation of copper ions (Cu^{2+}). Using the electrospinning technique, Xiao et al. immobilized the reactive ZVI into a polymeric matrix and showed its applicability to the removal of dyes from water [18].

In this present work, electrospinning technology was introduced to produce nZVI based carbonized nanofibers water filter synthesized via green method. The electrospun filters are supposed to be water stable, portable, and can be easily installed on domestic taps and pipes. The fabricated filters have a large surface to volume ratio, which provide many active sites for pollutant adsorption, allowing for enhanced removal of contaminants from water. Furthermore, the carbonization of the electrospun nanofibers enhances their durability and stability in water. The nZVI is employed to block heavy metal remediation and provide mechanical strength to nanofibers based water filters [19]. These methods improve filtration properties by tailoring nanofiber properties and promoting effective stabilization of nZVI in nanofibers structure. The green synthesis methods for nZVI in carbon nanofibers offers better control over nanoparticle size, shape, and distribution through electrospinning. There were no need to use high pressure, temperature, energy, and toxic chemicals in the fabrication of these filters [20]. The green synthesis methods minimize environmental impact and health hazards by using eco-friendly precursors and mild reaction conditions. The applied green synthesis method is biocompatible and potentially reliable for water filtration applications[21,22].

By employing the characterization techniques, we can gain a comprehensive insight into the structural, chemical, and physical properties of nZVI based nanofibrous mats. These understandings enable us to optimize synthesis processes, assess material quality, and tailor their applications accordingly. The scanning electron microscopy is used to examine the surface morphology and structure of nZVI based composites / carbonized nanofibrous mats. It provides high resolution images that reveal the arrangement of nanoparticles, the presence of impurities, and any defects within the material. The energy dispersive spectroscopy is often combined with SEM and determines elemental composition and distribution within the sample. The EDS can detect and analyze the characteristic X-rays emitted by a sample when it is bombarded with high energy electrons or other types of radiation. Thermogravimetric analysis measures the weight changes of a material as it is subjected to controlled temperature variations. It helps determine the thermal stability, decomposition temperature, and the presence of volatile components or impurities within the

Preprints (www.preprints.org) | NOT PEER-REVIEWED | Posted: 23 October 2023 doi:10.20944/preprints202310.1374.v1

sample. X-ray Diffraction provides information about the arrangement of atoms or molecules within a material including nanofibrous mats. By analyzing the diffraction pattern produced when X-rays interact with the sample, XRD can determine the crystal structure, phase composition, and crystallite size of the nanofibrous mats. FTIR analyzes the infrared absorption and transmission of a material. It helps identify the types of chemical bonds present, detect the presence of specific functional groups, and identify potential contaminants. FTIR spectra can provide valuable information about the chemical composition and molecular structure of nanofibrous mats. UV-Vis spectroscopy measures the absorption of ultraviolet and visible light by a material. It helps determine the absorption characteristics and bandgap properties of the nanofibrous mats. UV-Vis spectra can provide insights into the electronic structure and optical properties of the material.

2. Materials and Methods

2.1. Materials and Synthesis

For the fabrication of composite/carbon nanofibers, 90 grams of green tea (GT) was purchased from the local market, polyvinyl alcohol (PVA, Mw = 66,000) was supplied by Junsei Chemical, tetraethyl orthosilicate (TEOS, 98% purity) was purchased from Sigma Aldrich, ferric chloride hexahydrate ($FeCl_3.6H_2O$, molar mass = 270.3 gm/mol) was purchased from Doejung Co., Ltd. Distilled deionized water was used exclusively in all solution preparations and cleaning process, as shown in Table 1.

Table 1. Chemicals used in solution preparation for the fabrication of carbon nanofibers.

	Description	Brand
1	green tea, wt. = 90	Locally available
2	PVA, Mw = 66,000	Junsei
3	TEOS, 98% purity	Sigma Aldrich
4	$FeCl_3.6H_2O$, molar mass = 270.3 gm/mol	Doejung

The green tea solution was prepared by mixing 90 gm green tea in 500 ml of deionized water and heating it to 100 °C. For the fabrication of composite/carbonized nanofibers samples, the 20 ml of green tea solution was used as starting material and heated for 10 minutes on a hot plate at 60 °C. Then, 10 wt.% PVA/TEOS with a 7/3 weight ratio were mixed with the 20 ml of prepared green tea solution. The PVA was used as a dispersant or stabilizer agent, TEOS was added for more flexibility and mechanical strength required. The composite solution was stirred with the magnetic stirrer (KERN ALS 220-4) at 100 °C. The composite solution was stirred for 3 to 4 hours at 1000 rpm before being used, to make the solution homogeneous and gain suitable viscosity.

The freshly prepared composite solution of 10 mL was loaded into a syringe having a 21-gauge stainless steel needle. The flow rate of the solution was set at 1 mL/h through a syringe pump. The electrospinning voltage was kept at 20 kV and the distance from tip to collector was 10 cm. The collector was wrapped in aluminum foil, which acts as an opposite electrode. The composite nanofibers mats were finally dried in a vacuum oven (Thomas Scientific Model, 605) at 100 °C for 24 hours and then collected from aluminum foil. The dried composite nanofibers sample were kept in the crucible and carbonized in the tube furnace (Nabertherm Model, LHT 04 / 18) at 280 °C for 5 hours with a 3 °C/min rise in temperature. The carbonized nanofiber samples were kept in a desiccator before characterization.

For the fabrication of nZVI based composite / carbonized nanofibers sample, the 20 ml of green tea solution was used as starting material and heated for 10 minutes on a hot plate at 60 °C. Then, 10 wt.% PVA / TEOS with a 7/3 weight ratio were mixed into the 20 ml of prepared green tea solution. The PVA was used as a dispersant or stabilizer agent, TEOS was added for more flexibility and mechanical strength required. The composite solution was stirred on the magnetic stirrer (KERN ALS 220-4) at 1000 rpm and at 150 °C. After 15 minutes of continuous stirring, 2 ml of $FeCl_3.6H_2O$ was

 doi:10.20944/preprints202310.1374.v1

added drop by drop in the beaker until the solution becomes completely black. The nZVI-based composite solution was stirred at 1000 rpm for 4 to 5 hours at 150 °C before use to make the solution homogeneous and gain suitable viscosity.

The freshly prepared composite solution of 10 mL was loaded into a plastic syringe having a 19-gauge stainless steel needle. The flow rate of the solution was set at 0.8 mL/h through a syringe pump. The electrospinning voltage was kept at 20 kV and the distance from the tip to the collector was 8 cm. The collector was wrapped with aluminum foil and then with a silver mesh, which acts as the opposite electrode. The nZVI-based composite nanofibers mat was finally dried in a vacuum oven (Thomas Scientific Model, 605) at 100 °C for 24 hours and collected from silver mesh. The dried nZVI-based composite nanofibers sample were kept in the crucible and carbonized in the tube furnace (Nabertherm Model, LHT 04 / 18) at 280 °C for 4 hours and 40 minutes with a 3 °C/min rise in temperature. The nZVI-based carbonized nanofibers samples were kept in a desiccator before characterization.

2.2. Characterization Techniques

The morphologies of the fabricated composite / carbonized samples were observed through an SEM (JSM–5910LV, JEOL Ltd., Japan) with an operating voltage of 10 kV. The elemental composition of the nZVI-based composite or carbonized nanofibrous mats was analyzed by an EDX detector (INCA 200X, Oxford, U.K.). The TG / DT analysis was carried out using a Diamond series TG / DTA unit (Perkin Elmer Instruments Co., Ltd., USA) with a heating rate of 5 °C/min at the temperature range of 40 °C to 1000 °C. The X–ray diffraction pattern of the samples was carried out using a Rigaku Geiger flux X–ray Diffractometer with Cu Kα radiation (λ = 1.504 Å) operating at 40 kV. The FTIR spectra were recorded using a Nicolet 6700 FTIR spectrometer (Thermo Nicolet Corporation, US) at a wavenumber range of 4000-400 cm^{-1} at room temperature. The absorption spectra of nZVI-based carbonized nanofibers samples were recorded using a Perkin Elmer Lambda 1050 UV-Vis spectrophotometer in the spectral range of 200 nm–600 nm.

3. Results and Discussion

3.1. Morphological and Thermal Analysis

3.1.1. SEM Analysis of Composite and Carbonized Nanofibers

Figure 1 shows the SEM images of green tea composite and carbonized nanofibers with 10 wt.% PVA / TEOS (7/3 weight ratio) concentration. The nanofibers were fabricated using an electrospinning setup with a 10 ml syringe with a 21-gauge stainless steel needle. The distance between the syringe needle and the oppositely charged electrode was kept at 10 cm. The 18 kV voltage was applied, the flow rate of the solution was 1 ml/hr. The composite nanofibers were dried overnight at 100 °C in an oven and then collected on aluminum foil. The dried composite nanofibers were carbonized in the furnace at 280 °C for 5 hours with a temperature rise of 3 °C/min. The SEM images of the composite and carbonized nanofibers are taken at different resolutions of 1000 nm and 500 nm. The fabricated composite nanofibers as shown in Figure 1a,b are almost uniform in diameters of approximately 500 nm. The diameters of carbonized nanofibers were almost uniform and reduced to approximately 260 nm, as observed in Figure 1c,d. The reduction in diameters was due to the evaporation of the PVA contents after the carbonization of composite nanofibers. No beads or cracks were observed in the nanofiber structure. All the nanofibers were approximately of the same size, aligned and had no branches and pores.

Preprints (www.preprints.org) | NOT PEER-REVIEWED | Posted: 23 October 2023 doi:10.20944/preprints202310.1374.v1

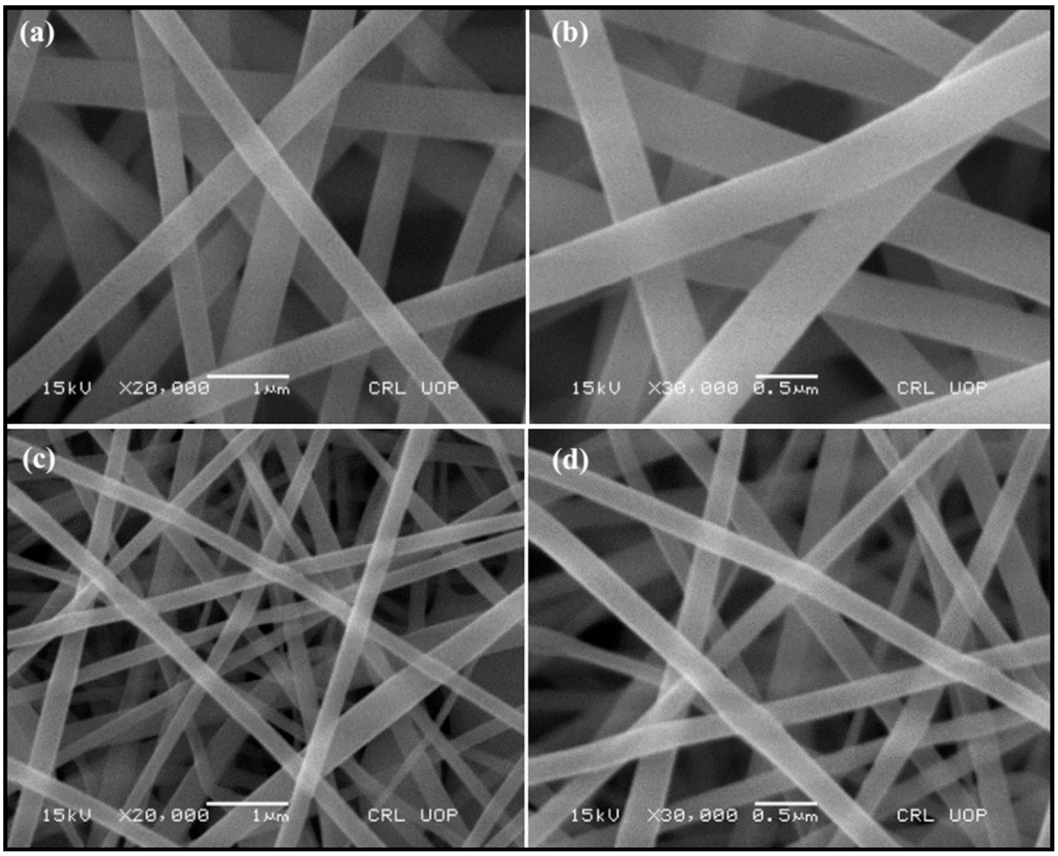

Figure 1. SEM images of (**a**,**b**) composite nanofibers and (**c**,**d**) carbonized nanofibers at 280 °C.

3.1.2. SEM and EDX Analysis of nZVI-Based Composite and Carbonized Nanofibers

Figure 2 shows the SEM and EDX analysis of nZVI-based green tea/PVA nanofibers from 10 wt.% PVA / TEOS (7/3 w/w). The iron precursor $FeCl_3.6H_2O$ was added drop by drop until the solution became completely black. The TEOS was added for flexibility and to give more mechanical strength to the fabricated nanofibers [23]. The nZVI-based green tea / PVA nanofibers were fabricated using an electrospinning setup with a 10 ml syringe and a 19-gauge stainless steel needle. The distance between the syringe needle and the oppositely charged electrode was kept at 10 cm. The 18 kV voltage was applied, the flow rate of the solution was 0.8 ml/hr for the fabrication of composite nanofibers. The nZVI-based composite nanofibers were dried overnight at 100 °C in an oven and collected on silver mesh and then carbonized at 280 °C. The SEM images of the nZVI-based nanofibers are taken at different resolutions of 1000 nm and 500 nm. The nZVI-based composite nanofibers as shown in Figure 2a,b are uniform in diameters of approximately 200 nm. No single beads and cracks, and all the composite nanofibers were aligned. The nZVI-based composite nanofibers were approximately the same in size and had no branches and pores.

With the incredible water solubility of PVA, the created nZVI-based composite nanofibers can be dissolved in water quickly, this is impossible for their use as a nanofilter for water treatment [24]. The treated dried composite nanofiber mats based on nZVI were heated at a temperature of 280 °C for 4 hours and 40 minutes with a gradual increase in temperature at a rate of 1 °C per minute, in order to maintain their porous structure when immersed in water. The resulting nZVI-based carbonized nanofibers mats were insoluble in water and used for water filtration applications. The smooth surface morphology of fabricated nZVI-based carbonized nanofibers is shown in Figure 2d,e, but some beads were due to high carbonization temperature. The average diameters of the nZVI-based carbonized nanofibers were not uniform and reduced to approximately 120 nm. The reduction in diameters is due to the evaporation of the PVA contents after the carbonization of nZVI-based composite nanofibers.

 doi:10.20944/preprints202310.1374.v1

EDX analysis of nZVI-based green tea / PVA composite nanofibers Figure 2c confirms the presence of elemental iron with chlorine and some oxygen which is due to the addition of $FeCl_3.6H_2O$ in solution. The presence of some oxygen is also due to the surface oxidation of nZVI-based green tea/PVA composite nanofiber in the air during handling and silicon is from the TEOS. The presence of the other elements including Na, P, and K due to the green tea solutions. The atomic and weight percentages of the different elements shown in the EDX analysis are recorded in Table 2.

EDX analysis of nZVI-based carbonized nanofibers at 280 °C Figure 2f confirms the presence of elemental iron with chlorine and some oxygen which is due to the addition of $FeCl_3.6H_2O$ in solution. The presence of some oxygen is also due to the surface oxidation of nZVI-based carbonized nanofiber in air during handling and silicon is from the TEOS. The presence of carbon is greater in weight due to the carbonization of organic materials and the disappearance of phosphorus and sodium is due to the carbonization temperature. The atomic percentages along with weight percentages of the different elements shown in EDX analysis are recorded in Table 3.

Table 2. EDX elemental analysis of nZVI-based composite nanofibers.

Element	Weight%	Atomic%
C	41.31	56.69
O	24.39	25.12
Na	4.32	3.10
Si	14.43	8.47
P	0.69	0.37
Cl	9.84	4.57
K	1.58	0.66
Fe	3.44	1.02
Total	100	100

Table 3. EDX elemental analysis of nZVI-based composite nanofibers at 280 °C.

Element	Weight%	Weight%
C	54.74	63.34
O	39.15	34.00
Si	3.76	1.86
Cl	1 1.25	0.49
K	0.34	0.12
Fe	0.77	0.19
Total	100	100

Preprints (www.preprints.org) | NOT PEER-REVIEWED | Posted: 23 October 2023 doi:10.20944/preprints202310.1374.v1

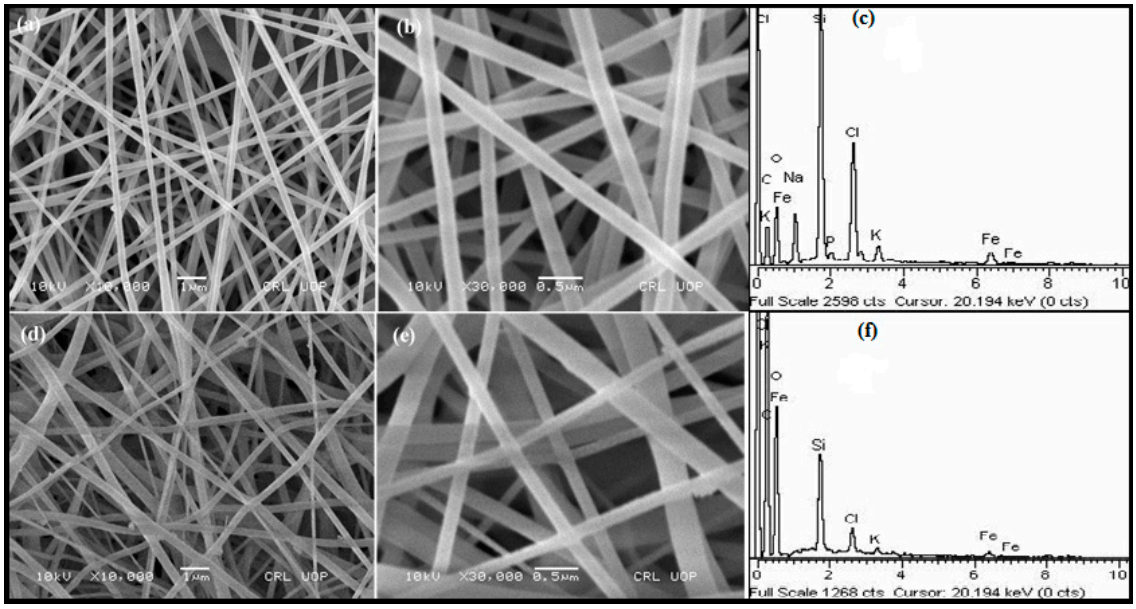

Figure 2. SEM images and EDX of zerovalent iron-based (**a** and **b**) composite and (**c** and **d**) carbonized nanofibers.

3.1.3. TG / DT Analysis of nZVI-Based Composite Nanofibers

Figure 3 shows the TG / DT analysis of nZVI-based composite nanofibers, with a sample weight of 8.969 mg. The sample was heated in the range of 40 °C to 1000 °C at 5 °C/min, under an N_2 atmosphere at a flow rate of 20 ml/min. It is clear from the TGA curve that there are three main stages of weight loss as a function of temperature and the total weight loss is about 94% in the range of 40 °C to 410 °C. In the first stage, the weight loss in the range of 40 °C to 100 °C is about 14%, which is due to the removal of moisture and volatile component present in nZVI-based composite nanofiber [18]. In the DTA curve, a small endothermic peak at 50 °C confirms the removal of moisture from the composite nanofiber and the weight remains constant from 70 °C to 180 °C. In the second stage, the weight loss in the range of 100 °C to 250 °C is almost 70%, which is caused by the degradation of PVA and removal of the Si–OH group present in nZVI-based composite nanofiber [25]. In the DTA curve, a sharp exothermic peak was observed at 250 °C due to the combustion of organic polymer present in nZVI-based composite nanofibers and regarded as the decomposition temperature of PVA. In the third stage, the weight loss in the range of 250 °C to 410 °C is about 10%, which is due to the complete removal of organic polymers present in nZVI-based composite nanofiber [26]. In the DTA curve, a very small exothermic peak at 400 °C also confirms the complete removal of organic polymers present in the nZVI-based composite nanofiber. Above 410 °C, there was no more weight loss and the TGA curve became stable, leaving behind pure nZVI-based nanofibers that accounted for approximately 6% of the weight. However, a slight endothermic decrease in the DTA curve showed the formation of nZVI-based nanofibers.

Preprints (www.preprints.org) | NOT PEER-REVIEWED | Posted: 23 October 2023 doi:10.20944/preprints202310.1374.v1

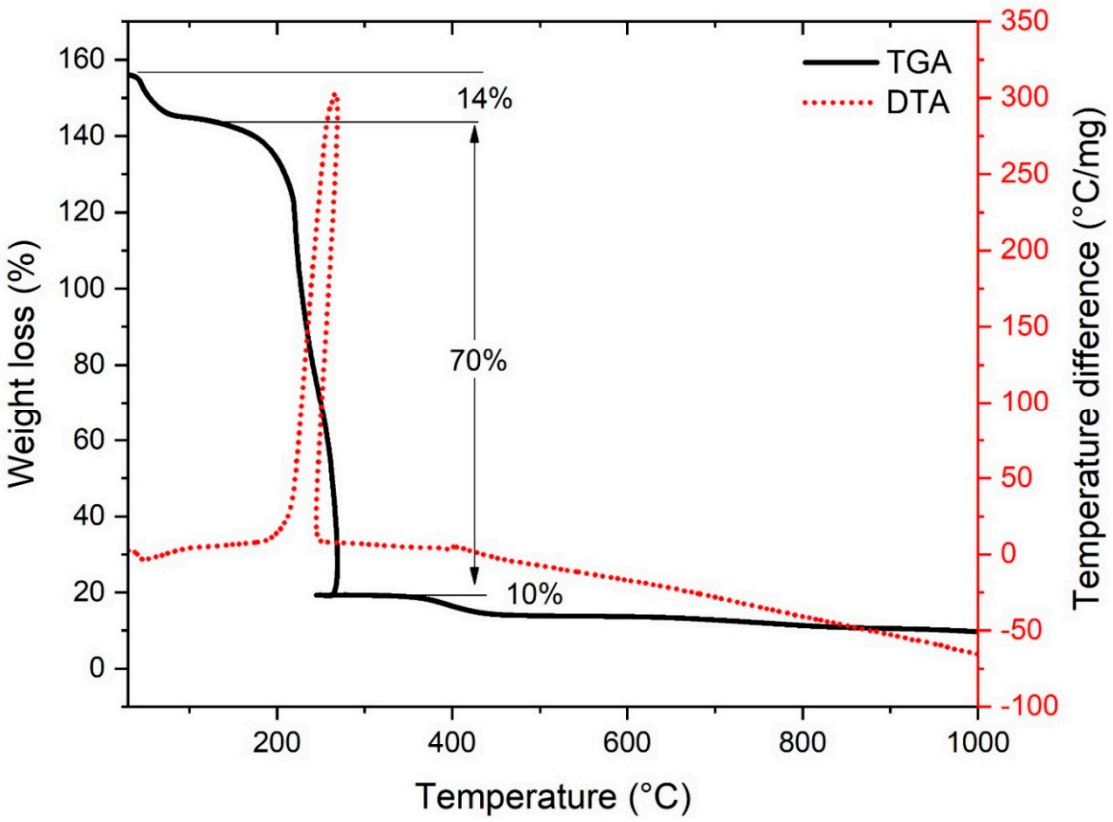

Figure 3. TG / DT analysis of nZVI-based composite nanofibers.

3.2. Phase and Structural Analysis.

3.2.1. XRD Analysis of nZVI-based Carbonized Nanofibers

Figure 4 shows the XRD analysis of the nZVI-based green tea / PVA composite nanofiber, carbonized at 280 °C. The XRD pattern of nZVI based carbonized nanofibers sample was recorded over a range of 10°-70°. The iron peaks (PDF Card No. 87-722) were observed at 2θ values of 44.7°, 66.9°. These peaks were consistent with that of the development of body-centered cubic iron crystallite in the nanofiber matrix. The peak at 2θ value of 44.7° ascribes to the formation of nZVI, confirmed the value of nZVI reported in the literature [27]. There were seven peaks of iron oxides (PDF Card No. 65-3107) at 2θ = 18.3°, 29.9°, 35.2°, 37.2°, 43.8°, 57.1°, 62.5°. These peaks suggested that the formation of iron oxide from the redox reaction between nZVI and oxygen in the environment after carbonization [28]. There were peaks of carbon (PDF Card No. 72-2091) at 2θ = 29.45°, 53.1°. These peaks suggested that the existence of carbon at the nanoscale from the carbonization of the nanofibers matrix [29]. PVA is semi-crystalline and the small intensity diffraction peaks of polymers, which are dominated by the presence of sharp peaks from iron nanoparticles.

Preprints (www.preprints.org) | NOT PEER-REVIEWED | Posted: 23 October 2023 doi:10.20944/preprints202310.1374.v1

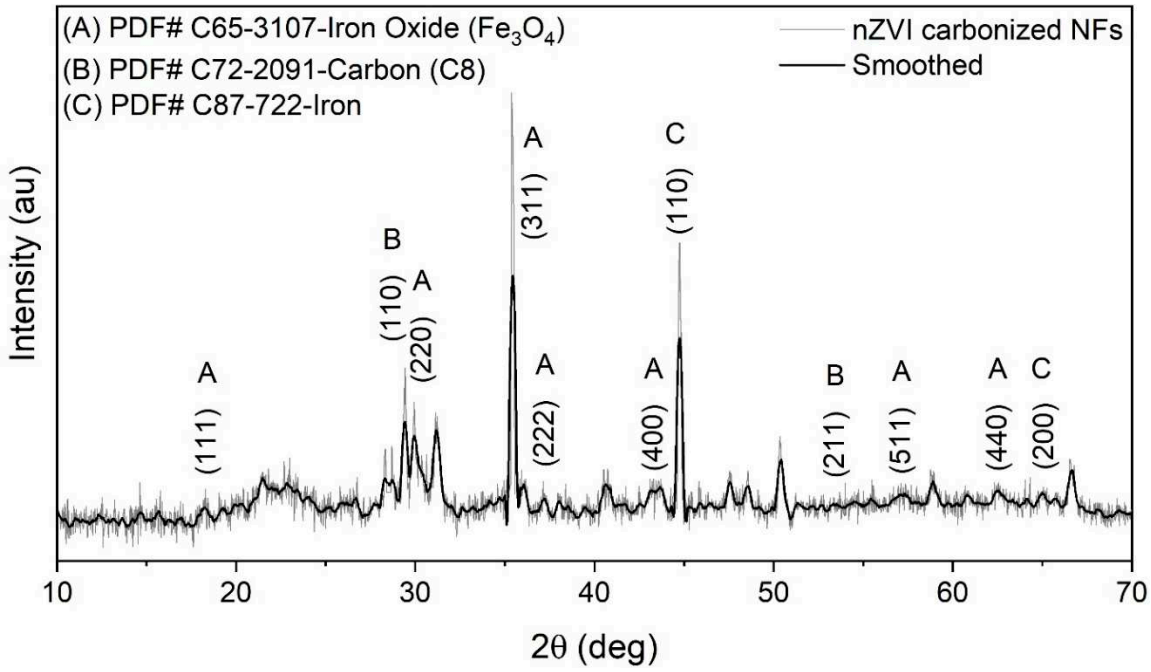

Figure 4. XRD pattern of nZVI-based carbonized nanofibers.

3.2.2. FTIR Analysis of Composite and Carbonized Nanofibers

Figure 5a shows the FTIR spectrum of PVA / GT composite and carbonized nanofibers in the range of 500-4000 cm^{-1}. The functional group region is successively from 4000-1500 cm^{-1}, and the fingerprint region from 1500-500 cm^{-1}. The fingerprint region is important because each different compound produces its own unique pattern of peaks in this region. In the spectrum of composite nanofibers, the broad absorption peak at 3280 cm^{-1} was due to the stretching vibration of O–H bonds in water molecules [30]. The absorption peak at 2915 cm^{-1} was due to the stretching vibration of C=H bonds in the alkanes chain of PVA molecules [31]. The absorption band from 2324 cm^{-1} to 1925 cm^{-1} was due to the presence of stretching vibration of C≡C bonds and a sharp peak at 1615 cm^{-1} was ascribed to the stretching vibration of C=C bonds, indicates the polyphenols present in the green tea extract [32]. The peaks at 1415 cm^{-1}, and 1319 cm^{-1} indicates the stretching vibration of CH_2 bond, and the peaks at 1230 cm^{-1} ascribes the stretching vibration of C–H bonds, which resulting the strong interaction between the hydroxyl group of PVA and GT extracts [33]. The peak at 1140 cm^{-1} is ascribes to the stretching vibration of C–C bonds, which indicates the crystalline region in the composite nanofibers sample [34]. The sharp peak at 1092 cm^{-1} matches with Si–O–Si vibration band, which shows the presence of TEOS in the composite nanofibers sample [35]. The peaks at 913 cm^{-1} and 838 cm^{-1} are allocated to the interactions between carboxylic groups (COO– asymmetric stretching) of PVA in the composite nanofibers structure. The less intense bands region from 570 cm^{-1}-500 cm^{-1} was due to the O–Si–O vibration, which shows the presence of TEOS in the composite nanofibers sample [36].

In the spectrum of carbonized nanofibers showed the O–H stretching vibration peak at 3453 cm^{-1} of bonded H_2O molecules (present in small quantity in the solid sample) with PVA. The shift in the peak from 3280 cm^{-1} (in composite nanofibers) to 3480 cm^{-1} and small intensity of the peaks was due to the vaporization of H_2O molecules. The vibration band at 2915 cm^{-1} (in composite nanofibers) of C–H stretching in alkanes appeared at 2909 cm^{-1} in the carbonized nanofibers spectrum, which was due to the decomposition of PVA molecules. The absorption band from 2359 cm^{-1}-1856 cm^{-1} was due to the presence of stretching vibration of C≡C bonds, indicates the presence of polyphenols in the green tea extract. The slight shift in the absorption band was due to the decomposition temperature of carbonized nanofibers [32]. The peak at 1711 cm^{-1} was due to the C–O stretches vibration from the remaining alcoholic group in carbonized nanofibers sample [37]. The peak at 1615 cm^{-1} of C=C

Preprints (www.preprints.org) | NOT PEER-REVIEWED | Posted: 23 October 2023 doi:10.20944/preprints202310.1374.v1

stretching vibration was slightly shifted to 1594 cm^{-1} due to the carbonization of composite nanofibers. The peaks at 1415 cm^{-1}, 1319 cm^{-1}, 1230 cm^{-1}, and 1140 cm^{-1} shown in the composite nanofiber spectrum were due to C–O and C–C stretching vibrations disappeared and a flat peak at 1367 cm^{-1} appeared due to C–C stretching vibration after carbonization. The sharp peak at 1106 cm^{-1} corresponds to the Si–O–Si stretching vibration but was slightly shifted due to carbonization. The absorption peaks at 872 cm^{-1} and less intense absorption bands from 755–600 cm^{-1} were attributed to the characteristic vibrations of Si–O–Si and C–Si asymmetric stretching in carbonized nanofibers samples, respectively [38].

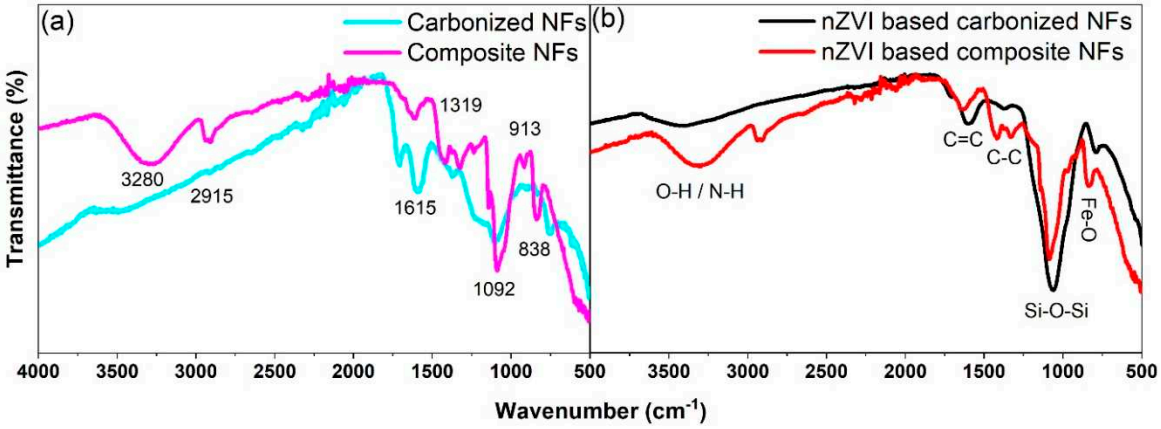

Figure 5. FTIR spectra of (**a**) composite and carbonized, (**b**) nZVI-based composite and carbonized nanofibers.

3.2.3. FTIR Analysis of nZVI-based Composite and Carbonized Nanofibers

Figure 5b shows the FTIR spectrum of the nZVI-based composite and carbonized nanofibers in the bands range of 500-4000 cm^{-1}. In the spectrum of nZVI-based composite nanofibers, the broad absorption peak at 3309 cm^{-1} is ascribed to O–H / N–H stretching vibration, which may be due to the H_2O molecules and polyphenols from GT extracts [39]. The absorption peak at 2922 cm^{-1} was due to C–H stretching vibration in alkanes present in the nZVI-based composite nanofibers sample [31]. The absorption band from 2359 cm^{-1} to 1884 cm^{-1} was due to the presence of C≡C stretching vibration and the peak at 1683 cm^{-1} was ascribed to the C=C stretching vibration, indicating the polyphenol present from GT extract coated onto the nZVI surface [40]. The peaks at 1421 cm^{-1} and 1326 cm^{-1} shown in nZVI based composite nanofibers sample was due to C–H stretching and bending vibration, which indicates the strong interaction between the CH_2 group of PVA and nZVI [41]. The sharp peak at 1082 cm^{-1} corresponds to Si–O–Si vibration band, which showed the presence of TEOS in the nZVI-based composite nanofibers sample [35]. The peaks at 966 cm^{-1}, 906 cm^{-1}, and 837 cm^{-1} are assigned to the interactions between nZVI and carboxylic groups (COO– asymmetric stretching) of PVA. The bands region from 596 cm^{-1} to 500 cm^{-1} was due to the Fe–O stretching vibration and Fe–O–Si stretching vibrations present in the nZVI-based composite nanofibers sample [39].

The spectrum of carbonized nanofibers showed a less intense peak at 3417 cm^{-1}, which was due to the O–H/N–H bending and stretching vibration of surface-absorbed H_2O molecules and polyphenols from GT extracts [39]. The shift in the peak from 3309 cm^{-1} (in nZVI-based composite nanofibers) to 3417 cm^{-1} and less intensity of the peaks ascribed to the vaporization of H_2O molecules present in the fibrous structure [41]. The absorption peak at 2922 cm^{-1} of C–H stretching vibration in alkanes disappeared in the nZVI-based carbonized nanofibers spectrum, which was due to the decomposition of PVA with carbonization temperature [31]. The absorption band from 2200 cm^{-1} to 1986 cm^{-1} ascribed the presence of C≡C stretching vibration, which was due to the interaction of polyphenol present from GT extract and nZVI on carbonized nanofibers surface [40]. The small peak appearing at 1713 cm^{-1} in the spectrum of nZVI based carbonized nanofibers sample can be attributed to the C=O stretching vibration, which indicates the interaction between PVA and GT extract [42]. The broad peak at 1605 cm^{-1} was due to C=C stretching vibration and a small peak at 1374 cm^{-1} was

 doi:10.20944/preprints202310.1374.v1

due to C–C stretching vibration, which appeared in nZVI based carbonized nanofibers sample [43]. The sharp absorption peak appeared at 1062 cm^{-1} corresponding to the Si–O–Si stretching vibration instead of 1082 cm^{-1} (in nZVI composite nanofibers sample), the shift in the peak was due to carbonization of the sample [44]. The absorption peak at 790 cm^{-1} is due to the presence of zerovalent iron nanoparticles in carbonized nanofibers samples, as reported in the literature [35]. The small adsorption peak at 539 cm^{-1} refers to Fe-O stretching vibration of Fe_3O_4 and Fe_2O_3, which confirms the existence of Fe nanoparticles in carbonized nanofibers samples [45].

Generally, these prescribed absorbance bands correspond with other research studies... Consequently, it can be presumed that the presence of different functional groups indicates the plausible reason for the formation and stabilization of synthesized nZVI in nanofibers structure. Hence amalgamation of nanoparticles is mainly expected due to the existence of polyphenolic compounds, which will directly reduce iron ions to zerovalent particles [46].

3.3. Absorption Spectroscopy Analysis

3.3.1. UV-Vis Analysis of Composite, Carbonized Nanofibers and nZVI-based Composite, Carbonized Nanofibers

Figure 6 shows the absorption spectra of composite, carbonized, and nZVI-based composite, carbonized nanofibers samples, which were dispersed in deionized water. The absorption spectra were taken in the wavelength range from 200 nm to 800 nm for observing surface plasmon resonance. Some of the organic compounds and transition metal ions show absorption spectra in the ultraviolet (190-400 nm) or visible (400-900 nm) regions of electromagnetic radiation. The conduction band and valence band in metal nanoparticles are very near to each other in which electrons freely move. The free electrons give rise to surface plasmon resonance absorption, occurring due to the collective oscillation of electrons in resonance with light waves [47]. The wavelength absorption peak at 272 nm in the composite nanofiber spectrum was typical to the GT extracts, which correspond to the tea polyphenols and caffeine and confirmed the interaction with PVA [13,43]. The absorption peak at 245 nm in carbonized nanofiber also confirmed the presence of polyphenols and caffeine from GT. The less intensity of the peak showed the degradation of PVA due to the temperature [43]. The PVA / GT composite solution containing $FeCl_3.6H_2O$ exhibit black color, which was due to the excitation of surface plasmon resonance of iron nanoparticles. Therefore, the reduction of iron nanoparticles into nZVI nanoparticles during interaction with GT extracts in electrospun nanofibers can be followed by UV-Vis spectroscopy. The absorption spectra were taken in the wavelength range from 200 nm to 800 nm for observing the reduction of Fe^{+3} ions to Fe^0. The wavelength absorption peak at 272 nm in nZVI based composite nanofibers spectrum was typical of the GT extract. The intensity of the peaks declined after reacting with iron when the reaction between $FeCl_3$ and green tea extracts led to the solution color changing rapidly from yellow to dark. This indicated that it was due to polyphenols and caffeine acted as reducing agents in the process of iron nanoparticles produced by tea extracts [43]. The absorption band from 215 nm to 260 nm was shown in nZVI based carbonized nanofibers spectrum, which confirmed the surface plasmon resonance at 215 nm of synthesizing nZVI in nanofibers structure. The shifting of surface plasmon resonance peaks toward the lower wavelength region was due to temperature, which also showed the confirmation of nZVI [48]. Green tea extracts such as catechins and polyphenols have been studied for their potential to synthesize nZVI based on the indication of surface plasmon resonance with absorption peaks under the visible region. The UV-Vis spectrum of the synthesized nZVI-based carbonized nanofibers was in accordance with what was reported in the range of 216 nm to 268 nm [49].

Preprints (www.preprints.org) | NOT PEER-REVIEWED | Posted: 23 October 2023 doi:10.20944/preprints202310.1374.v1

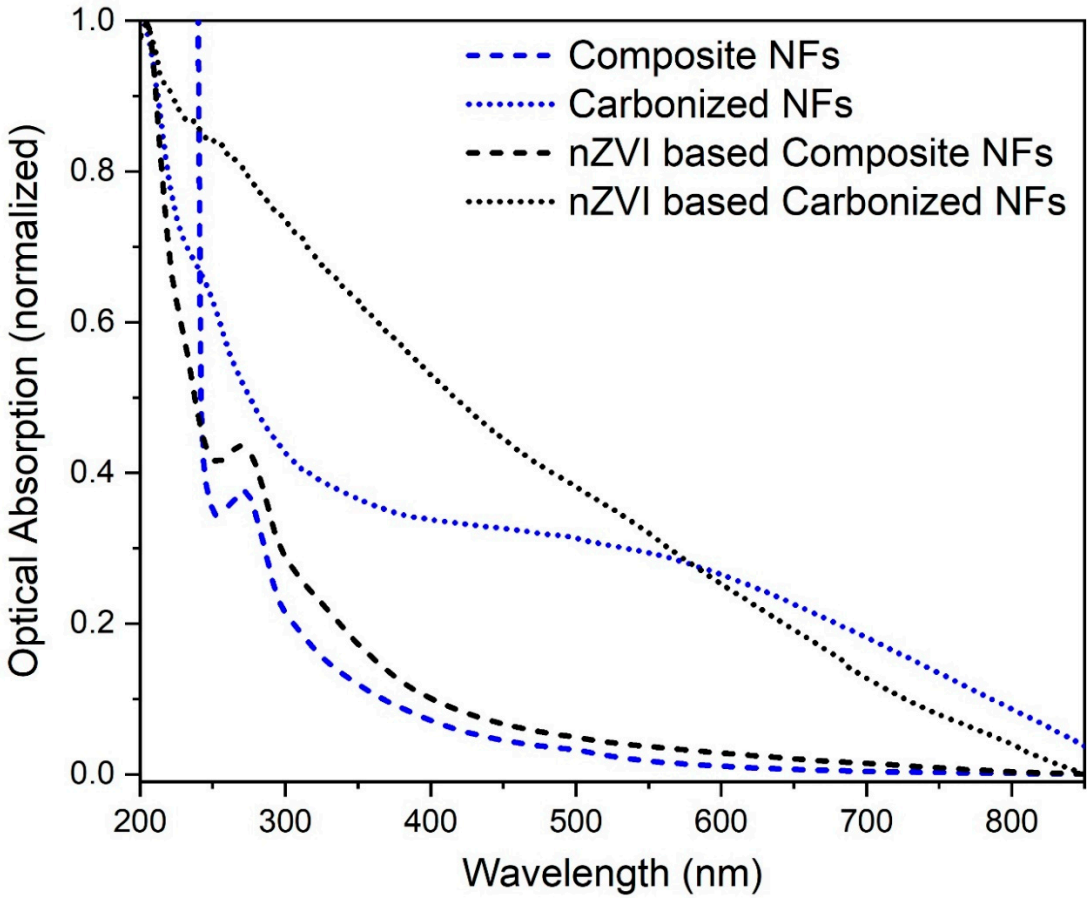

Figure 6. UV-Vis spectra of composite, carbonized, and nZVI-based composite, carbonized nanofibers.

4. Conclusions

This study presents the green synthesis of eco-friendly nZVI-based carbon nanofibers using the electrospinning technique for nanofiltration applications. The smooth and porous, nZVI-based carbon nanofibers were produced by carbonizing the as-spun composite nanofibers at 280 °C. The PVA / TEOS (7/3 wt.%) was used in 20 ml of green tea solution, for the optimization of nZVI-based composite nanofibers. The PVA concentration and temperature played a key role in the fabrication and morphology such as homogeneity, porosity, and uniformity in the diameter of nZVI-based composite / carbonized nanofibers. The TEOS also played a vital role in the nanofiber morphology, it gave more flexibility and mechanical strength to nZVI-based composite / carbonized nanofibers. Green tea was used as environmentally friendly and economical in the production of nZVI-based composite nanofibers. The SEM analysis showed that the nZVI-based composite nanofibers were uniform in diameters approximately equal to 200 nm and had a smooth surface. The diameter of nZVI-based composite nanofibers was reduced approximately to 120 nm after carbonization at 280 °C and had a smooth surface but was not uniform. The EDX analysis of nZVI-based carbon nanofibers indicated the presence of metallic iron at the nanoscale at 280 °C. The presence of Na, Cl, O, C, Fe, Si, and K peaks in EDX spectra also indicated the constituent elements in nZVI-based carbon nanofibers. The TG/DT analysis of nZVI-based composite nanofibers confirmed the complete removal of organic polymers at 280 °C. The weight became constant after 280 °C and the total loss in weight was about 94%. The XRD analysis of nZVI-based composite nanofibers showed that there is no crystallinity in the nanofibers structure. After carbonization at 280 °C, the XRD pattern of nZVI-based carbon nanofibers confirmed the formation of a single-phase nZVI. The XRD pattern of the nZVI-based carbon nanofibers was observed to be a single-phase cubic structure. The broad peaks in the XRD pattern indicated the presence of the nanocrystalline structure of the nanofibers. The FTIR spectra of

the prepared samples showed the numbers of peaks are less in the nZVI-based carbon nanofibers as compared to composite nanofibers, which indicated the removal of PVA and other organic contents from the nanofibers structure. The peaks in the FTIR spectra showed the presence of different functional groups, indicating the formation and stabilization of nZVI in the nanofiber structures. The absorbance peaks in the FTIR spectra indicated the presence of organic compounds (polyphenolic), which showed the direct reduction of iron ions into nZVI. The absorption peaks in the UV-Vis spectra, specifically at 215 nm to 268 nm in the wavelength range of 200 nm to 600 nm, correspond to the excitation of surface plasmon vibrations associated with the presence of nZVI. The large band intensities and absorption peaks in the visible region further indicate the successful formation of nZVI within the nanofiber structures.

Acknowledgment: The authors acknowledge the financial support by the Pakistan Science**;** Foundation (PSF-NSFC-IV-28) and Higher Education Commission of Pakistan**;** (Project NRPU-8148-2017).

References

1. S.M. Ponder, J.G. Darab, T.E. Mallouk, Remediation of Cr(VI) and Pb(II) Aqueous Solutions Using Supported, Nanoscale Zero-valent Iron, Environmental Science & Technology, 34 (2000) 2564-2569.
2. [2] J. Liu, C. Wang, J. Shi, H. Liu, Y. Tong, Aqueous Cr(VI) reduction by electrodeposited zero-valent iron at neutral pH: Acceleration by organic matters, Journal of Hazardous Materials, 163 (2009) 370-375.
3. C.-B. Wang, W.-x. Zhang, Synthesizing nanoscale iron particles for rapid and complete dechlorination of TCE and PCBs, Environmental science & technology, 31 (1997) 2154-2156.
4. Y. Liu, T. Phenrat, G.V. Lowry, Effect of TCE concentration and dissolved groundwater solutes on NZVI-promoted TCE dechlorination and H2 evolution, Environmental science & technology, 41 (2007) 7881-7887.
5. J. Fatisson, S. Ghoshal, N. Tufenkji, Deposition of carboxymethylcellulose-coated zero-valent iron nanoparticles onto silica: roles of solution chemistry and organic molecules, Langmuir, 26 (2010) 12832-12840.
6. B.I. Kharisov, H.R. Dias, O.V. Kharissova, A. Vázquez, Y. Pena, I.J.R.A. Gomez, Solubilization, dispersion and stabilization of magnetic nanoparticles in water and non-aqueous solvents: recent trends, 4 (2014) 45354-45381.
7. S. Wang, M. Zhao, M. Zhou, Y.C. Li, J. Wang, B. Gao, S. Sato, K. Feng, W. Yin, A.D. Igalavithana, P. Oleszczuk, X. Wang, Y.S. Ok, Biochar-supported nZVI (nZVI/BC) for contaminant removal from soil and water: A critical review, Journal of Hazardous Materials, 373 (2019) 820-834.
8. L. Duan, Y. Dai, L. Shi, Y. Wei, Q. Xiu, S. Sun, X. Zhang, S.J.C. Zhao, Humic acid addition sequence and concentration affect sulfur incorporation, electron transfer, and reactivity of sulfidated nanoscale zero-valent iron, 294 (2022) 133826.
9. M. Li, Y. Mu, H. Shang, C. Mao, S. Cao, Z. Ai, L. Zhang, Phosphate modification enables high efficiency and electron selectivity of nZVI toward Cr(VI) removal, Applied Catalysis B: Environmental, 263 (2020) 118364.
10. T. Pasinszki, M.J.N. Krebsz, Synthesis and application of zero-valent iron nanoparticles in water treatment, environmental remediation, catalysis, and their biological effects, 10 (2020) 917.
11. Y.-P. Sun, X.-Q. Li, W.-X. Zhang, H.P. Wang, A method for the preparation of stable dispersion of zero-valent iron nanoparticles, Colloids and Surfaces A: Physicochemical and Engineering Aspects, 308 (2007) 60-66.
12. F. He, D. Zhao, Manipulating the size and dispersibility of zerovalent iron nanoparticles by use of carboxymethyl cellulose stabilizers, Environmental science & technology, 41 (2007) 6216-6221.
13. G.E. Hoag, J.B. Collins, J.L. Holcomb, J.R. Hoag, M.N. Nadagouda, R.S. Varma, Degradation of bromothymol blue by 'greener' nano-scale zero-valent iron synthesized using tea polyphenols, Journal of Materials Chemistry, 19 (2009) 8671-8677.
14. S.M. Ponder, J.G. Darab, J. Bucher, D. Caulder, I. Craig, L. Davis, N. Edelstein, W. Lukens, H. Nitsche, L. Rao, D.K. Shuh, T.E. Mallouk, Surface Chemistry and Electrochemistry of Supported Zerovalent Iron Nanoparticles in the Remediation of Aqueous Metal Contaminants, Chemistry of Materials, 13 (2001) 479-486.
15. B. Kim, H. Park, S.-H. Lee, W.M. Sigmund, Poly(acrylic acid) nanofibers by electrospinning, Materials Letters, 59 (2005) 829-832.
16. G.R. Del Sorbo, G. Truda, A. Bifulco, J. Passaro, G. Petrone, B. Vitolo, G. Ausanio, A. Vergara, F. Marulo, F. Branda, Non Monotonous Effects of Noncovalently Functionalized Graphene Addition on the Structure and Sound Absorption Properties of Polyvinylpyrrolidone (1300 kDa) Electrospun Mats, in: Materials, 2019.

17. S. Xiao, H. Ma, M. Shen, S. Wang, Q. Huang, X. Shi, Excellent copper(II) removal using zero-valent iron nanoparticle-immobilized hybrid electrospun polymer nanofibrous mats, Colloids and Surfaces A: Physicochemical and Engineering Aspects, 381 (2011) 48-54.
18. S. Xiao, M. Shen, R. Guo, S. Wang, X. Shi, Immobilization of zerovalent iron nanoparticles into electrospun polymer nanofibers: synthesis, characterization, and potential environmental applications, The Journal of Physical Chemistry C, 113 (2009) 18062-18068.
19. M. Gui, V. Smuleac, L.E. Ormsbee, D.L. Sedlak, D.J.J.o.N.R. Bhattacharyya, Iron oxide nanoparticle synthesis in aqueous and membrane systems for oxidative degradation of trichloroethylene from water, 14 (2012) 1-16.
20. K. Krishnaswamy, H. Vali, V.J.J.o.F.E. Orsat, Value-adding to grape waste: Green synthesis of gold nanoparticles, 142 (2014) 210-220.
21. V. Guarino, V. Iannotti, G. Ausanio, L. Ambrosio, L. Lanotte, Elastomagnetic nanofiber wires by magnetic field assisted electrospinning, Express Polymer Letters, 13 (2019) 419-428.
22. V. Guarino, V. Iannotti, G. Ausanio, L. Ambrosio, L. Lanotte, Nanocomposite tubes for magneto-active devices, Express Polymer Letters, 14 (2020) 651-662.
23. M.H. Tai, P. Gao, B.Y.L. Tan, D.D. Sun, J.O.J.A.a.m. Leckie, interfaces, Highly efficient and flexible electrospun carbon–silica nanofibrous membrane for ultrafast gravity-driven oil–water separation, 6 (2014) 9393-9401.
24. Y. Zou, X. Wang, A. Khan, P. Wang, Y. Liu, A. Alsaedi, T. Hayat, X.J.E.s. Wang, technology, Environmental remediation and application of nanoscale zero-valent iron and its composites for the removal of heavy metal ions: a review, 50 (2016) 7290-7304.
25. M. Stefănescu, M. Stoia, O. Stefănescu, C. Davidescu, G. Vlase, P.J.R.R.C. Sfîrloagă, Synthesis and caracterization of poly (vinylalcohol)/ethylene glycol/silica hybrids. Thermal analysis and FT-IR study, 55 (2010) 17-23.
26. U.K. Fatema, A.J. Uddin, K. Uemura, Y.J.T.R.J. Gotoh, Fabrication of carbon fibers from electrospun poly (vinyl alcohol) nanofibers, 81 (2011) 659-672.
27. B.D. Iverson, S.V.J.M. Garimella, nanofluidics, Recent advances in microscale pumping technologies: a review and evaluation, 5 (2008) 145-174.
28. J.-F. Gao, H.-Y. Li, K.-L. Pan, C.-Y.J.R.a. Si, Green synthesis of nanoscale zero-valent iron using a grape seed extract as a stabilizing agent and the application for quick decolorization of azo and anthraquinone dyes, 6 (2016) 22526-22537.
29. R. Sharma, D.S. Rao, V.J.M.L. Vankar, Growth of nanocrystalline β-silicon carbide and nanocrystalline silicon oxide nanoparticles by sol gel technique, 62 (2008) 3174-3177.
30. T. Wang, X. Jin, Z. Chen, M. Megharaj, R.J.S.o.t.t.e. Naidu, Green synthesis of Fe nanoparticles using eucalyptus leaf extracts for treatment of eutrophic wastewater, 466 (2014) 210-213.
31. G. Vázquez, E. Fontenla, J. Santos, M. Freire, J. González-Álvarez, G.J.I.c. Antorrena, products, Antioxidant activity and phenolic content of chestnut (Castanea sativa) shell and eucalyptus (Eucalyptus globulus) bark extracts, 28 (2008) 279-285.
32. S. Gunalan, R. Sivaraj, V.J.P.i.N.S.M.I. Rajendran, Green synthesized ZnO nanoparticles against bacterial and fungal pathogens, 22 (2012) 693-700.
33. M. Wrona, M.J. Cran, C. Nerín, S.W.J.C.p. Bigger, Development and characterisation of HPMC films containing PLA nanoparticles loaded with green tea extract for food packaging applications, 156 (2017) 108-117.
34. H. Tadokoro, K. Kŏzai, S. Seki, I.J.J.o.P.S. Nitta, On the crystalline band in the infrared absorption spectrum of polyvinyl alcohol, 26 (1957) 379-382.
35. S. Wen, L. Liu, L. Zhang, Q. Chen, L. Zhang, H.J.M.L. Fong, Hierarchical electrospun SiO2 nanofibers containing SiO2 nanoparticles with controllable surface-roughness and/or porosity, 64 (2010) 1517-1520.
36. T. Chen, Z. Wu, W. Wei, Y. Xie, X.A. Wang, M. Niu, Q. Wei, J.J.R.a. Rao, Hybrid composites of polyvinyl alcohol (PVA)/Si–Al for improving the properties of ultra-low density fiberboard (ULDF), 6 (2016) 20706-20712.
37. H.S. Mansur, C.M. Sadahira, A.N. Souza, A.A.J.M.S. Mansur, E. C, FTIR spectroscopy characterization of poly (vinyl alcohol) hydrogel with different hydrolysis degree and chemically crosslinked with glutaraldehyde, 28 (2008) 539-548.
38. Q. Zhu, Y. Chu, Z. Wang, N. Chen, L. Lin, F. Liu, Q.J.J.o.M.C.A. Pan, Robust superhydrophobic polyurethane sponge as a highly reusable oil-absorption material, 1 (2013) 5386-5393.
39. X. Weng, L. Huang, Z. Chen, M. Megharaj, R.J.I.C. Naidu, Products, Synthesis of iron-based nanoparticles by green tea extract and their degradation of malachite, 51 (2013) 342-347.
40. K.L. Garner, S. Suh, A.A.J.E.S. Keller, Technology, Assessing the risk of engineered nanomaterials in the environment: development and application of the nanoFate model, 51 (2017) 5541-5551.
41. A. Singhal, M. Kaur, K. Dubey, Y. Bhardwaj, D. Jain, C. Pillai, A.J.R.a. Tyagi, Polyvinyl alcohol–In 2 O 3 nanocomposite films: synthesis, characterization and gas sensing properties, 2 (2012) 7180-7189.

 doi:10.20944/preprints202310.1374.v1

42. X.H. Qin, S.Y.J.J.o.A.P.S. Wang, Electrospun nanofibers from crosslinked poly (vinyl alcohol) and its filtration efficiency, 109 (2008) 951-956.
43. L. Huang, X. Weng, Z. Chen, M. Megharaj, R.J.S.A.P.A.M. Naidu, B. Spectroscopy, Green synthesis of iron nanoparticles by various tea extracts: comparative study of the reactivity, 130 (2014) 295-301.
44. F. He, S. Chao, X. He, M.J.C.I. Li, Inorganic microencapsulated core/shell structure of Al–Si alloy microparticles with silane coupling agent, 40 (2014) 6865-6874.
45. M. Iram, C. Guo, Y. Guan, A. Ishfaq, H.J.J.o.h.m. Liu, Adsorption and magnetic removal of neutral red dye from aqueous solution using Fe3O4 hollow nanospheres, 181 (2010) 1039-1050.
46. V. Smuleac, R. Varma, S. Sikdar, D.J.J.o.m.s. Bhattacharyya, Green synthesis of Fe and Fe/Pd bimetallic nanoparticles in membranes for reductive degradation of chlorinated organics, 379 (2011) 131-137.
47. S. Basavaraja, S. Balaji, A. Lagashetty, A. Rajasab, A.J.M.R.B. Venkataraman, Extracellular biosynthesis of silver nanoparticles using the fungus Fusarium semitectum, 43 (2008) 1164-1170.
48. M.J.J.N.R. Sivakumar, SCG Kiruba Daniel, G. Vinothini, N. Subramanian, K. Nehru &, 15 (2013) 1-10.
49. A. Sebastian, A. Nangia, M.J.P.o.t.N.A.o.S. Prasad, India Section A: Physical Sciences, Green Synthesis of Iron Nanoparticles from Selected Plant Materials of Peninsular India, 88 (2018) 195-203.